



Investigation of antifouling properties of polypropylene/TiO₂ nanocomposite membrane under different aeration rate in membrane bioreactor system

Habib Etemadi^{a,*}, Milad Fonouni^{b,c}, Reza Yegani^{b,c,**}

^a Department of Polymer Science and Engineering, University of Bonab, Bonab, Iran

^b Faculty of Chemical Engineering, Sahand University of Tehnology, Tabriz, Iran

^c Membrane Technology Research Center, Sahand University of Technology, Tabriz, Iran

ARTICLE INFO

Article history:

Received 25 April 2019

Received in revised form 9 October 2019

Accepted 30 December 2019

Keywords:

Membrane bioreactor

Aeration rate

Polypropylene membrane

Antifouling

ABSTRACT

This paper presents the results of aeration rate effect on antifouling properties of polypropylene (PP)/TiO₂ nanocomposite membrane in membrane bioreactor (MBR) system in order to oil refinery wastewater treatment. For this purpose, three levels of aeration rate with specific aeration demand per membrane area (SADm) of 0.5, 1, and 1.5 m³/m²h was used. According to the obtained results, PP nanocomposite membrane showed high hydrophilicity, porosity, and high flux compared to neat PP membrane. Also, either low or high aeration rate had a negative influence on permeability and antifouling properties of neat PP and nanocomposite membranes. The analysis of fouling mechanism for both membranes based on Hermia's model revealed that the cake formation is dominant mechanism for lower aeration rate while by increasing aeration rate, all models couldn't predict experimental data. Meanwhile, by increasing aeration rate, chemical oxygen demand (COD) removal for activated sludge and both membranes decreased and increased, respectively.

© 2019 The Authors. Published by Elsevier B.V. This is an open access article under the CC BY license (<http://creativecommons.org/licenses/by/4.0/>).

1. Introduction

Today water scarcity is a serious problem all over the world due to the increasing in population and the expansion of industry activities [1]. Therefore, it seems that wastewater treatment and reuse are necessary. Among several wastewater reuse and recycling processes, membrane-based technologies show great potential to overcome water scarcity [2]. In this case, membrane bioreactor (MBR) technology widely used for the treatment of various municipal and industrial wastewater, because of small footprint demand and high quality of effluent compared to other conventional wastewater treatment systems [3,4]. However, membrane fouling and prohibitively costly compared with the more established conventional technologies is the major problem impeding the widespread adoption of MBR to full-scale plants [5–7].

According to the literature, two strategies including of operational conditions and membrane modification was widely used to improvement in antifouling properties of membrane in MBR system. Among operational conditions, many studies have been focused on the effect of aeration rate on the membrane fouling. It is well known that the aeration intensity strongly impacts the mixed liquor organic matter fractions and correspondingly influences the membrane fouling rate [8]. Ivanovic et al. [9] showed that the relationship between sufficient aeration to minimize membrane fouling. Also, they proposed an approach to define optimal operating conditions with respect to aeration rates. Meng et al. [10] investigated the effect of aeration rate on membrane fouling in submerged MBR. They concluded that aeration had a positive effect on cake layer removal, but pore blocking became severe as aeration intensity increased to 800 L/h. In other words, under low aeration rate, foulants on the membrane surface was not removed effectively, while, high aeration could induce a severe breakage of sludge flocs.

Among all modification methods in membrane preparation, nanocomposite membranes demonstrate promising performances and are predicted to gather the intrinsic properties of both polymeric and inorganic membranes and give interesting advantages of the hybrid membrane such as great thermal and chemical resistances, good antifouling and separation performances, and

* Corresponding author.

** Corresponding author at: Faculty of Chemical Engineering, Sahand University of Tehnology, Tabriz, Iran.

E-mail addresses: h_etemadi@ubonab.ac.ir (H. Etemadi), ryegani@sut.ac.ir (R. Yegani).

excellent adaptation to the severe operating conditions [11]. In this regard various nanoparticles were used in order to improvement in antifouling properties of membrane in MBR systems.

On the other hand, using low cost membrane such as polypropylene (PP), can reduce the MBR costs. PP are good candidates for preparation of membrane due to high mechanical strength, high chemical stability, thermal resistance and low cost [11,12]. Therefore, PP is a very promising material for separating membranes. Although the prepared PP membrane exhibit many advantages, it still has several disadvantages, such as low porosity, poor hydrophilicity and high fouling [12,13]. The disadvantages reduce the water flux of the PP membrane and limit applications of this membrane in wastewater treatment applications. Therefore, it seems that PP membrane modification is essential in order to using in MBR system. For this purpose, as mentioned above, incorporation of hydrophilic nanoparticles into polymer matrix is one of the effective methods to enhance the membrane antifouling properties. Among different inorganic nanoparticles, titanium dioxide (TiO₂) has received most of the attention because of its unique specifications such as stability under harsh conditions, commercial availability and easiness of preparation.

In our previous work [13], PP/TiO₂ nanocomposite membrane was prepared via thermally induced phase separation (TIPS) method and it was tested in MBR system. However, in the current work, the effect of aeration rate on antifouling properties of PP/TiO₂ nanocomposite membrane was investigated using oil refinery wastewater influents obtained from Tabriz Oil Refinery Co. in MBR system. In this case, the fouling mechanism as well as antifouling performance of both fabricated membrane (neat and nanocomposite membranes) was investigated.

2. Experimental

2.1. Materials

Isotactic PP with commercial grade (EPD60R) was supplied from Arak Petrochemical Co., Iran. The melt flow index of PP was 0.35 g/10 min. TiO₂ nanoparticles (particle size of ca. 21 nm) were purchased from Sigma- Aldrich (Germany). Mineral oil as diluent, acetone as extracting agent and Irganox 1010 as heat stabilizer were purchased from Acros Organics (Belgium), Merck (Germany) and Ciba Co. (Switzerland), respectively. All materials were used as-received unless otherwise described.

2.2. Membrane preparation

The neat PP and nanocomposite membrane was fabricated by TIPS method using a sealed glass vessel kept in silicone oil bath. A certain amount of TiO₂ nanoparticles (0.75 wt.%) with Irganox (1 wt% of solid phase) were dispersed into 60 g of mineral oil using bath sonication (Woson, China) for 60 min. Then, PP was added to the diluent-TiO₂ suspension and melt blended at 170 °C for 90 min. The solution was then allowed to degas for 30 min and cast on a preheated glass sheet using a doctor blade with the film thickness of 250 μm. The plate was immediately quenched in the water bath (30 ± 3 °C) to induce phase separation. The membrane was then immersed in acetone for 24 h to extract its diluent.

2.3. Membranes characterization

The microscopic morphology of the neat PP and nanocomposite membranes was characterized by scanning electron microscope (SEM) (VEGA3, TESCAN). The hydrophilic properties

of membranes was evaluated by measuring the contact angle between membrane surface and water droplet using a goniometer (PGX, Thwing-Albert Instrument Co., USA). All reported data of contact angle are the average of five different tests from each membrane sample.

Membrane porosity was measured using gravimetric method. In this method, PP membranes were immersed in i-butanol for 24 h and then immediately weighed after removing i-butanol from the surface. The porosity was calculated using the following equation [12]:

$$\varepsilon(\%) = \frac{(W_{wet} - W_{dry})/D_i}{(W_{wet} - W_{dry})/D_i + W_{dry}/D_p} \times 100 \quad (1)$$

where W_{dry} is the initial membrane weight, W_{wet} is the membrane weight after 24 h immersion in i-butanol, D_p and D_i are the density of PP (0.91 g/cm³) and i-butanol (0.8 g/cm³), respectively.

Tensile strength of the membranes was analyzed via tensile test machine (STM-5, SANTAM) at an extension rate of 50 mm/min. At least three measurements were carried out and the mean value for each case was reported.

The tortuosity (τ) of the membrane was determined using Eq. (2) [14]:

$$\tau = \frac{(2 - \varepsilon)^2}{\varepsilon} \quad (2)$$

2.4. MBR set-up

In this study, a lab-scale submerge MBR (12 L working volume) was used. The flat sheet membrane modules had a volume of 50 mL and an effective membrane filtration area of 14.7 cm². Fig. 1 shows flat sheet modules submerged in the MBR test system. An air diffuser was installed beneath the membrane module to provide dissolved oxygen as well as efficient agitation of activated sludge in the MBR. Transmembrane pressure (TMP) was maintained constant at 0.1 bar. Mixed liquor suspended solid (MLSS) concentration was about 7000 mg/l. Hydraulic retention time (HRT) and sludge residence time (SRT) were maintained at 24 h and 20 days, respectively.

Real wastewater with chemical oxygen demand (COD) of 178 mg/l was supplied from Tabriz Oil Refinery Company (TZ.O.R.C), Tabriz, Iran. The literature showed that air injection reduced fouling in an submerged MBR up to a critical flow rate corresponding to a specific aeration demand per membrane area (SADm) of 0.25 m³/m² h [15,16]. Therefore, in this study, the lower value of SADm was corresponding to 0.5 m³/m² h. The effect of aeration rate on the membrane fouling was examined, and in this case, SADm was selected for three different rates; 0.5, 1, and 1.5 m³/m² h.

2.5. Antifouling performance of membranes

Antifouling performance of neat PP and PP/TiO₂ (0.75 wt.%) membranes were evaluated by filtrating activated sludge. After pure water flux tests (J_{w1} , L/m²h), filtration experiments were carried out for 360 min at 0.1 bar and the flux for activated sludge (J_{AS} , L/m²h) was measured. Then the membrane was taken out for simple cleansing under running deionized water and the pure water flux of cleaned membranes J_{w2} (L/m²h) was measured again. The flux recovery ratio (FRR) was calculated as follows:

$$FRR(\%) = \frac{J_{w2}}{J_{w1}} \times 100 \quad (3)$$

Furthermore, the antifouling property of membranes was also evaluated by the total fouling ratio (TFR), reversible fouling ratio

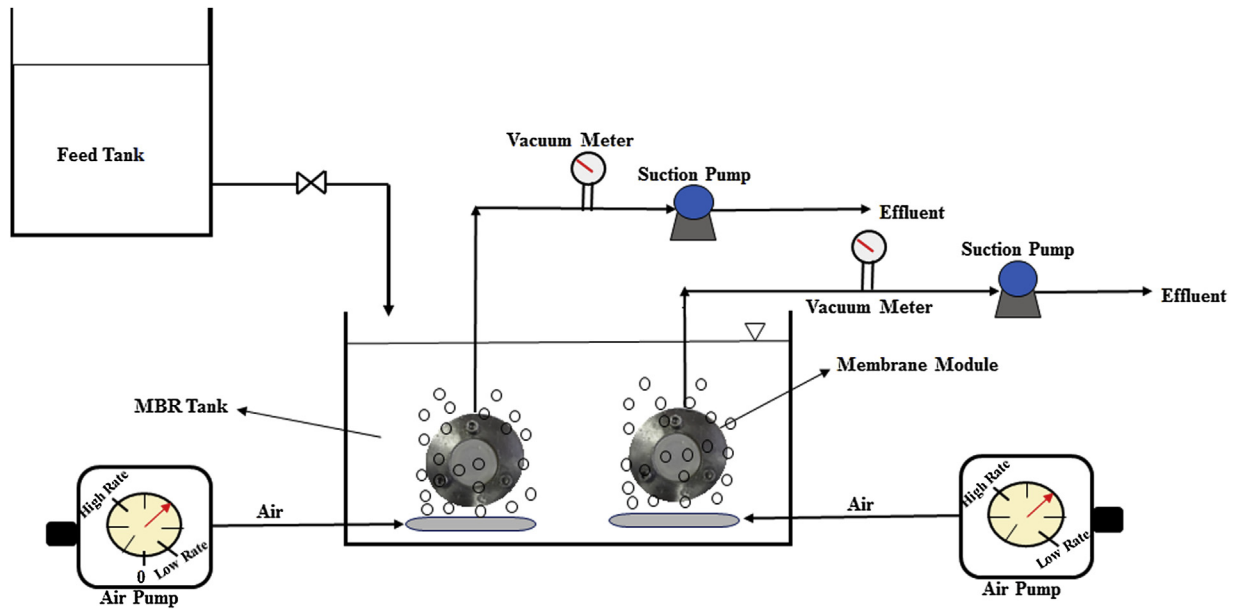


Fig. 1. Schematic of MBR setup in this study.

(RFR) as well as irreversible fouling ratio (IFR) according to the following equations [4,17]:

$$RFR(\%) = \left(\frac{J_{w2} - J_{AS}}{J_{w1}} \right) \times 100 \quad (4)$$

$$IFR(\%) = \left(\frac{J_{w1} - J_{w2}}{J_{w1}} \right) \times 100 \quad (5)$$

$$TFR(\%) = RFR(\%) + IFR(\%) = \left(\frac{J_{w1} - J_{AS}}{J_{w1}} \right) \times 100 \quad (6)$$

COD removal was estimated by measuring COD of effluent (COD_E) and influent (COD_I) based on absorbance method as described elsewhere [18] and using the following equation [18]:

$$COD\text{Removal}(\%) = \left(1 - \frac{COD_E}{COD_I} \right) \times 100 \quad (7)$$

2.6. Analysis of fouling mechanisms

According to Hermia's model, under constant pressure filtration condition, four fouling mechanisms blamed for flux decline could be explained using the following mathematical equation [19]:

$$\frac{d^2t}{dV^2} = k \left(\frac{dt}{dV} \right)^m \quad (8)$$

where t (h) is filtration time, V (m^3) is the filtrate volume, k is the resistance coefficient and specific formulation of these fouling mechanisms could be characterized with different values of m : $m = 0$ for cake filtration, $m = 1$ for intermediate blockage, $m = 1.5$ for standard blockage and $m = 2$ for complete blockage [20]. Using the flux expression (Eq. (9)), the flux decline expression can be expressed by Eq. (10):

$$J = \frac{1dV}{Adt} \quad (9)$$

$$\frac{dJ}{dt} = -kA^{2-m}j^{3-m} \quad (10)$$

In Eqs. (9) and (10), A is the effective membrane area (m^2).

3. Results and discussion

3.1. Membrane morphology

SEM images of surface of neat PP and PP/TiO₂ (0.75 wt.%) membranes, is shown in Fig. 2a and b. By addition of TiO₂ nanoparticles the nucleation density and porosity increased in PP nanocomposite membrane when compared with neat PP membrane. In other words, due to the fact that TiO₂ nanoparticles acted as the crystal nuclei and a certain amount of TiO₂ dosage could increase the number of spherulites, decrease the size of spherulites and caves between the spherulites and make spherulites more uniform. Similar results was found in elsewhere [11]. Fig. 2a and b also show that the addition of TiO₂ nanoparticles increased the number and the size of pores in the surface of membrane. This may be due to the heterogeneous nucleation effect of TiO₂ nanoparticles.

Fig. 2c and d show the SEM images of cross section of membranes. From the SEM images of cross section it can be seen that the both membrane has sponge like porosity and symmetric structure.

3.2. Hydrophilicity, porosity and tensile strength of membranes

The results of contact angle measurement which is responsible for membranes hydrophilicity, are shown in Table 1. It can be seen that the hydrophilicity of PP membrane improved with the addition of TiO₂ nanoparticles in which the water contact angle decreases. The relatively higher hydrophilicity was found for PP/TiO₂ nanocomposite membranes due to the presence of hydroxyl functional groups on the TiO₂ nanoparticle surface [21].

Overall porosities of the fabricated membranes are presented in Table 1. By addition of 0.75 wt.% of nanoparticles, the porosity of PP membrane increased from 31.48 % to 50.74 % decreasing its pore tortuosity. Addition of TiO₂ nanoparticles could accelerate the crystallization rate and act as the crystal nuclei at the low quenching temperature [22], the average pore size and the porosity of nanocomposite membrane could be higher than those of the neat PP membrane.

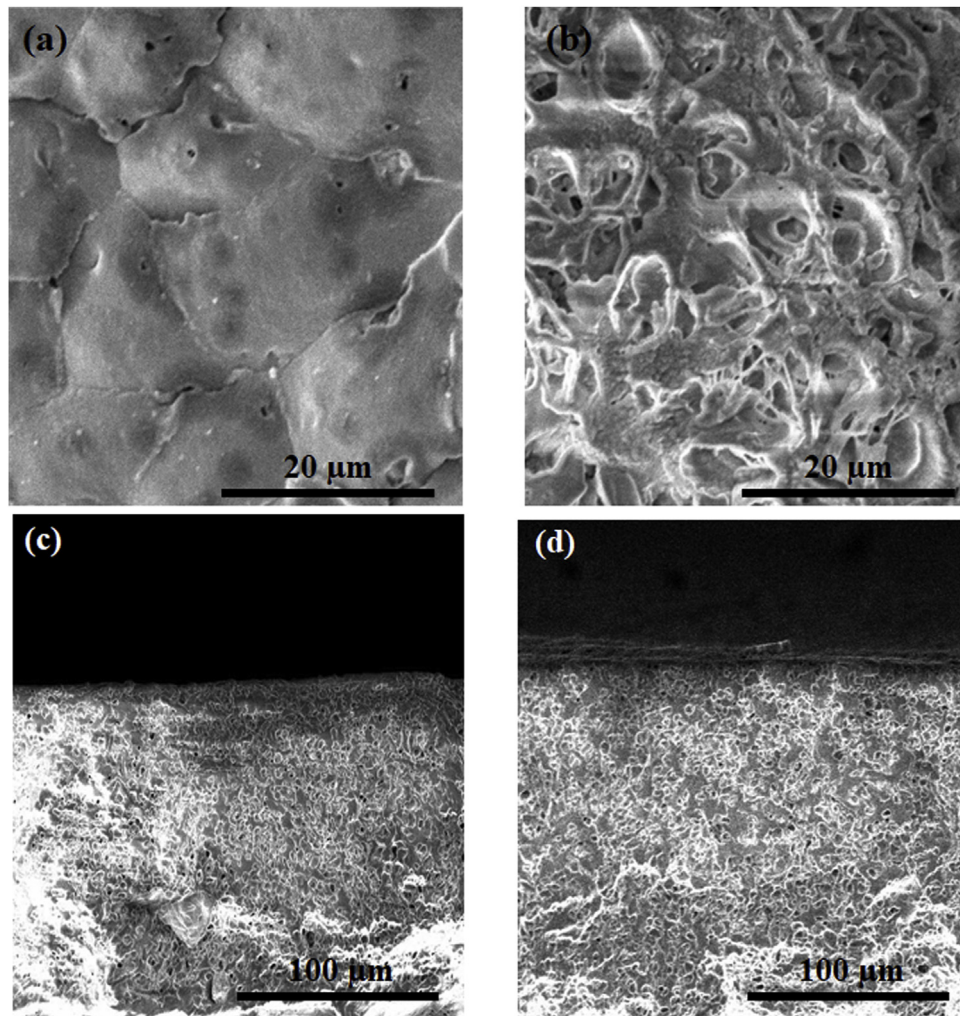


Fig. 2. SEM images of membrane surface of (a) neat PP, (b) PP/TiO₂ and cross section of (c) neat PP and (d) PP/TiO₂ membranes.

The tensile strength of neat PP and nanocomposite membrane are shown in Table 1. According to the obtained results, the tensile strength of neat PP membrane increased by following the addition of nanoparticle. Similar to our previous findings [23], this manner can be attributed to the crystallinity change in PP and the reinforcement effect of the inorganic nanoparticles due to the addition of nanoparticle

3.3. Fouling analysis and membrane performance

In order to evaluate the effect of aeration rate on antifouling properties of neat PP and PP/TiO₂ (0.75 wt.%) membrane, the permeate flux is plotted against time in Fig. 3 for various SADm, i.e. 0.5, 1, and 1.5 m³/m²h under TMP of 0.1 bar. As shown in Fig. 4a and b, for both membranes, flux at the end of filtration was decreased in the extreme low and high aeration rates. By increasing SADm from 0.5 to 1 m³/m²h and for both membranes, the flux through the

membrane increased at the whole of permeation time. At higher aeration rates, i.e. 1.5 m³/m²h, membrane permeability decreased. The results confirm the importance of aeration as a means to mitigate fouling in immersed membrane systems.

By comparing Fig. 3a and b, it is clear that the in comparison with neat PP membrane and for all aeration rates, flux has increased for nanocomposite membrane. That indicates that the membrane hydrophilicity and porosity as well as surface pore size (according to SEM images) played the vital role in the improvement of the activated sludge flux.

Fouling analysis was made by calculating the reversible fouling ratio (RFR), irreversible fouling ratio (IFR), total fouling ratio (TFR), and flux recovery ratio (FRR) of membranes under different aeration rates after activated sludge filtration test. These parameters are shown in Fig. 4. A higher FRR shows a better flux recovery while a lower IFR demonstrates a better performance controlling the total fouling [24]. In the aeration rate of 1 m³/m²h, the neat PP

Table 1

Water contact angle, porosity, tortuosity and tensile strength of neat PP and nanocomposite membranes.

Membrane type	Water contact angle (°)	Porosity (%)	Tortuosity	Tensile strength (MPa)
Neat PP	122.2	31.5	9.0	4.1
PP/TiO ₂ (0.75 wt.%)	106.0	50.7	4.4	4.7

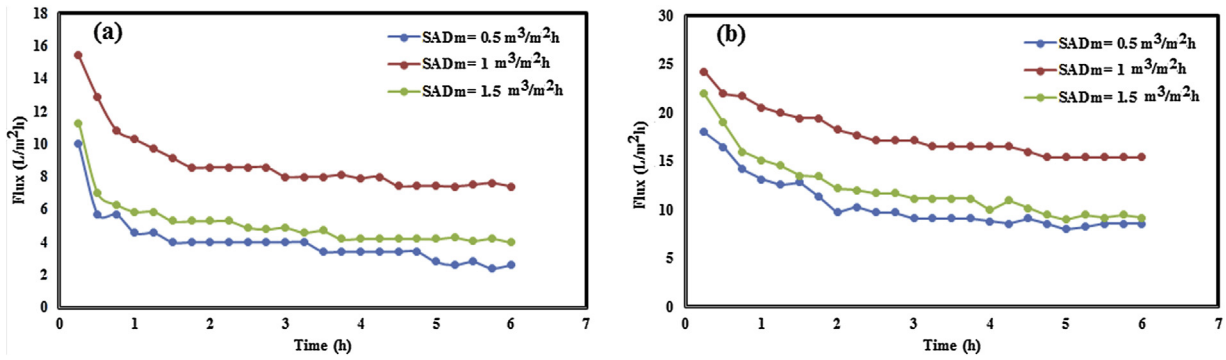


Fig. 3. Flux decline with operation time for (a) neat PP and (b) PP/TiO₂ membranes under different aeration rates and TMP = 0.1 bar.

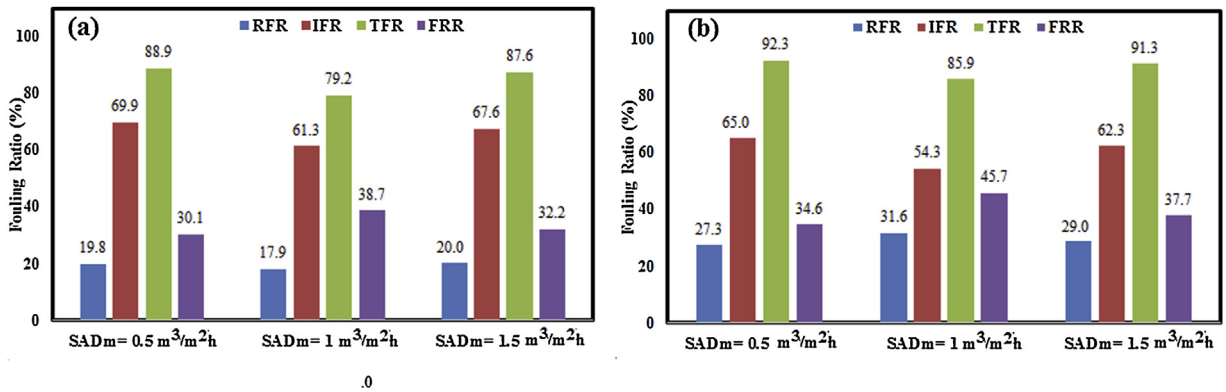


Fig. 4. Effect of aeration rates on fouling parameters of (a) neat PP and (b) PP/TiO₂ membranes.

and PP nanocomposite membrane shows the lowest IFR and TFR among other aeration rates. The IFR values for neat PP membrane were calculated to be 69.9 % and 61.3 % when the SADm were 0.5 and 1 m³/m²h, respectively (see Fig. 4a). Also, the values for FRR were 30.1, 38.7 %, and 32.2 % for SADm of 0.5, 1, and 1.5 m³/m²h, respectively. Similar trend was found for PP nanocomposite membrane under different aeration rates (see Fig. 4b).

Higher aeration rates more efficiently remove the fouling deposition or cake layer on the membrane surface due to the higher shear force of bubble air, and simultaneously increases the breakage of components that have been identified as major contributors to fouling. Therefore, under high aeration rates, the membrane fouling intensifies. Meanwhile, the small matters from

the occurrence of floc and particle breakage can penetrate the membrane pores, during which membrane pore blockage or irreversible fouling occurs. Fig. 5 shows the microscopic images of sludge flocs in mixed liquor under low (SADm = 0.5 m³/m²h) and high (SADm = 1.5 m³/m²h) aeration rates. It is clear that a low aeration rate results in larger floc and particles sizes, while a higher aeration rate creates smaller particle and flocs due to the floc breakage [25,26].

Comparing the RFR and IFR values of the neat PP and PP/TiO₂ membranes however, shows that the RFR and IFR values of the nanocomposite membrane are higher and lower than the neat PP membrane, respectively, which confirms the improvement of the antifouling property of nanocomposite membrane due to

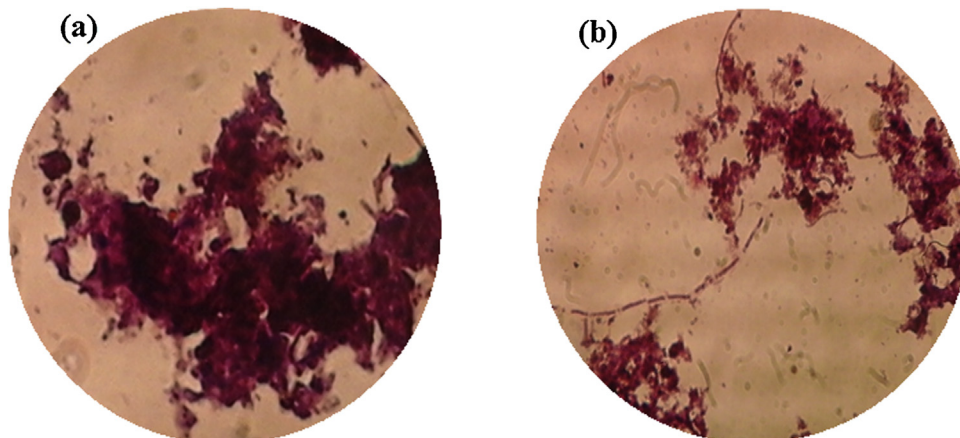


Fig. 5. Microscopic images of sludge flocs in mixed liquor under: (a) lower (SADm = 0.5 m³/m²h) and (b) higher (SADm = 1.5 m³/m²h) aeration rates.

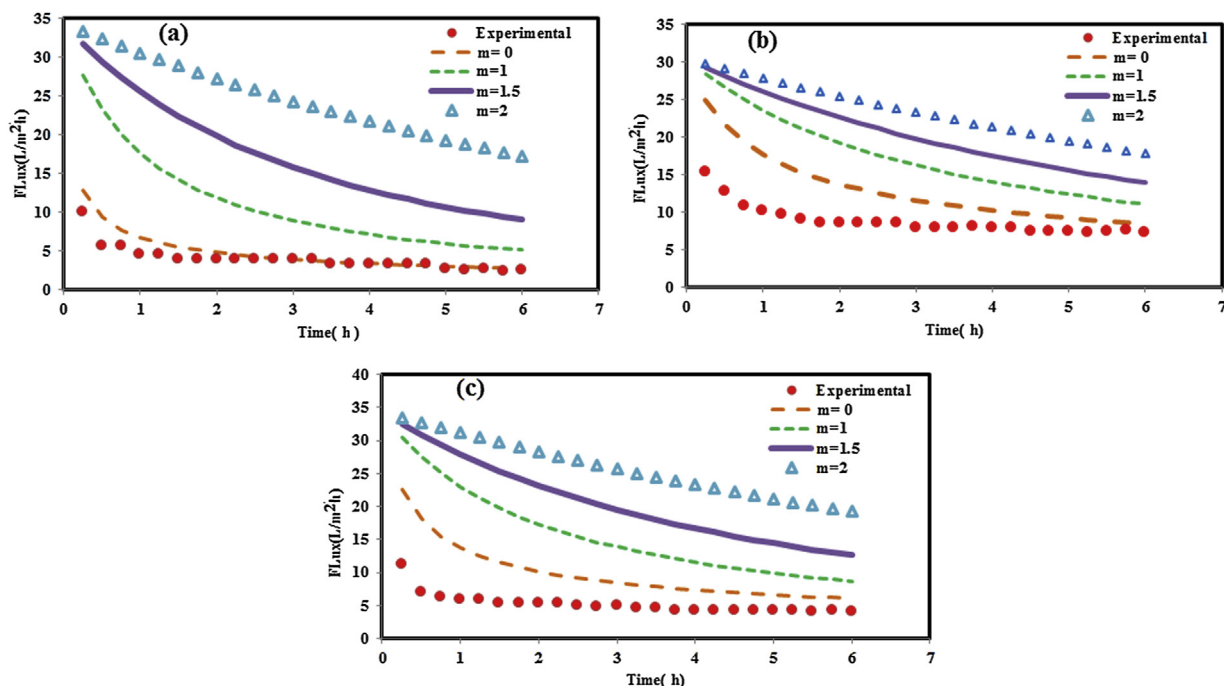


Fig. 6. Experimental data and Hermia fouling models for neat PP membrane under different aeration rates: (a) $SADm = 0.5 \text{ m}^3/\text{m}^2\text{h}$, (b) $SADm = 1 \text{ m}^3/\text{m}^2\text{h}$, and (c) $SADm = 1.5 \text{ m}^3/\text{m}^2\text{h}$.

hydrophilicity improvement. Generally, if the foulants (such as colloidal particles, sludge flocs and cell debris) are weakly bound on the membrane surface or within its pores, reversible fouling occurs, which can be easily eliminated by water rinsing. While, irreversible fouling occurs, when the foulants are strongly attached within the pores or membrane surface and chemical cleaning is seriously needed to remove these reagents [27,28]. Therefore, it seems that reduction in IFR is important for membrane separation process due to chemical cleaning and subsequently resulting in high cost.

Fig. 6 illustrates the fitting of the obtained experimental data after using the neat PP membrane in MBR system under various aeration rate conditions to different predicted fouling mechanisms, including complete pore blocking ($m = 2$), standard pore blocking ($m = 1.5$), intermediate pore blocking ($m = 1$), and cake formation ($m = 0$). In this study, in order to identify the mechanism of fouling during activated sludge filtration, the model k parameter was estimated by linear regression method. The adjusted values of k and correlation coefficient; R^2 , for $m = 0, 1, 1.5$, and 2 were used to solve the respective Hermia's equations and the obtained results are shown in Table 2. According to Fig. 6a, it is observed that under lower aeration rate ($SADm = 0.5 \text{ m}^3/\text{m}^2\text{h}$), a cake filtration model provides the best fit with neat PP membrane.

In Hermia's model, according to Zhang et al. [29] study, a k -value can be used to estimate the degree of membrane fouling. As shown in Table 2 and for neat PP membrane, for cake formation

model, the increased k values under different aeration rates follow the following order: $SADm = 1.5 \text{ m}^3/\text{m}^2\text{h} < SADm = 1 \text{ m}^3/\text{m}^2\text{h} < SADm = 0.5 \text{ m}^3/\text{m}^2\text{h}$, which indicates that the thickness of cake layer formed on the membrane surface under different aeration rates and for neat PP membrane is: $SADm = 1.5 \text{ m}^3/\text{m}^2\text{h} < SADm = 1 \text{ m}^3/\text{m}^2\text{h} < SADm = 0.5 \text{ m}^3/\text{m}^2\text{h}$. Therefore, as shown in the Fig. 6, cake filtration mechanism is the dominant mechanism for neat PP membrane under lower aeration rate ($SADm = 0.5 \text{ m}^3/\text{m}^2\text{h}$). Similar trend was found for PP/TiO₂ nanocomposite membrane (see Fig. 7a).

As shown in Figs. 6 and 7, by increasing in aeration rate from 0.5 to 1 and $1.5 \text{ m}^3/\text{m}^2\text{h}$, there is no model to quite well prediction of experimental data. These results indicated that the aeration rate largely determines the potential for floc breakage and release of small fragments into the bulk liquid which cause membrane pore blockage. As shown in Fig. 4, increasing in aeration rate (higher than $SADm$ of $2 \text{ m}^3/\text{m}^2\text{h}$) results in irreversible fouling. Under lower aeration rate, due to larger size of sludge floc and other particles, these matters accumulated on the membrane surface and cake layer formed on the membrane surface which can easily remove physically or eliminated by water rinsing. However, under very high aeration rate ($SADm = 1.5 \text{ m}^3/\text{m}^2\text{h}$) the floc and particle breakage occurs which these small matters can penetration through the membrane pores and membrane pore blockage or irreversible fouling occurs.

Table 2

Obtained k and correlation coefficient R^2 values for Hermia fouling models under different aeration rates for neat PP and nanocomposite membranes.

Membranes $SADm$ ($\text{m}^3/\text{m}^2\text{h}$)	$m = 0$		$m = 1$		$m = 1.5$		$m = 2$	
	k	R^2	k	R^2	k	R^2	k	R^2
0.5	0.021	0.947	0.038	0.867	0.037	0.841	0.151	0.783
PP 1	0.007	0.921	0.011	0.804	0.014	0.751	0.088	0.709
1.5	0.005	0.861	0.020	0.825	0.023	0.790	0.109	0.691
0.5	0.019	0.914	0.010	0.838	0.017	0.793	0.113	0.751
PP/TiO ₂ (0.75 wt.%) 1	0.004	0.879	0.004	0.792	0.008	0.687	0.069	0.682
1.5	0.003	0.870	0.009	0.841	0.017	0.801	0.122	0.770

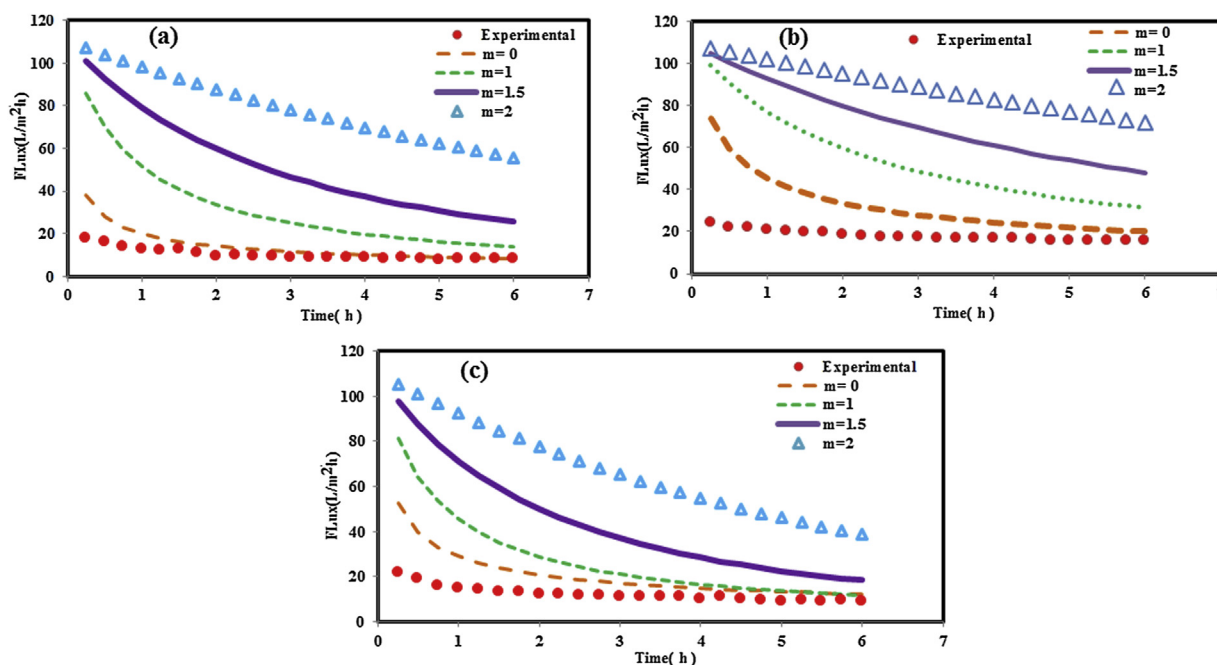


Fig. 7. Experimental data and Hermia fouling models for PP/TiO₂ nanocomposite membrane under different aeration rates: (a) SADm = 0.5 m³/m²h, (b) SADm = 1 m³/m²h, and (c) SADm = 1.5 m³/m²h.

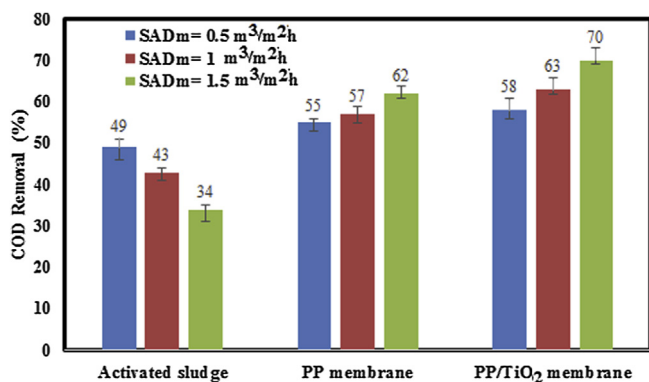


Fig. 8. COD removal for activated sludge and membranes under different aeration rates.

The amount of COD removal for activated sludge and membranes under different aeration rates was also investigated and the obtained results were shown in Fig. 8. It can be observed that COD removal of activated sludge decreased by increasing aeration rate. According to the Meng et al. [10] and Temmerman

et al. [25] studies, high aeration rates led to the release of soluble microbial products (SMP) and breakage of particles and bacteria. Therefore, it is expected that COD removal efficiency of activated sludge was decreased by increasing aeration rates. This trend was observed elsewhere [30]. However, COD removal increased by increasing aeration rate for neat PP and PP/TiO₂ membranes. As shown in Fig. 8, the higher COD removal for both membranes was appeared at the highest aeration rate (SADm = 1.5 m³/m²h). It could be concluded that high aeration rate results in breakage of particles and bacteria, and as mentioned previously, under high aeration rate membrane pore blockage occurs and foulants cannot cross through the membrane and therefore membrane COD removal increased. In other words, under high aeration rate conditions, due to the floc breakage, membrane pore blockage as well as thinner and denser cake layer was formed on the membrane surface and this phenomenon acts as a secondary membrane that filters and prevents the penetration of foulants [31]. On the other hand, under lower aeration rate conditions, due to the presence of larger sludge floc in MBR tank, a thicker and porous cake layer was formed on the membrane surface which cause foulants cross a cake layer and membrane and subsequently results in increasing COD with respect to higher aeration rate. This phenomenon schematically is shown in Fig. 9.

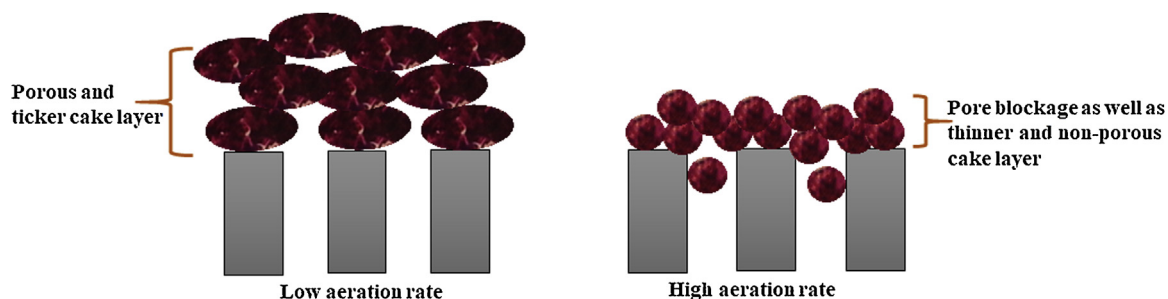


Fig. 9. Schematic illustration of biofilm formation and pore blockage for membrane under lower and higher aeration rates.

Comparing the COD removal values for neat PP and PP/TiO₂ membranes show that the COD removal for nanocomposite membrane was higher than neat membrane. This efficient reduction in COD can be ascribed to the presence of TiO₂ nanoparticle which results in increasing in membrane hydrophilicity.

4. Conclusions

This study examined the effect of aeration rate on antifouling properties of polypropylene/TiO₂ nanocomposite membrane in MBR system in order to oil refinery wastewater treatment. PP/TiO₂ nanocomposite membranes with high hydrophilicity and high porosity were successfully fabricated via TIPS method. The obtained results indicated low or high aeration rate had a negative influence on membrane permeability. Low aeration could not remove the membrane foulants from membrane surface effectively. However, high aeration could induce a severe breakage of sludge flocs. The SADm of 1 m³/m²h was selected as optimal aeration rate for both neat PP and nanocomposite membranes, which low IFR and high FRR was occurred.

According to the results obtained from Hermia's model, it can be determined that for both membranes, the best fit to experimental values are cake formation mechanism under lower aeration rate (SADm = 0.5 m³/m²h). However, by increasing aeration rate no one of models couldn't predict experimental data. Also, the COD removal rates for activated sludge decreased as the aeration rate increased. While, by increasing aeration rate, COD removal for neat PP and PP/TiO₂ membranes increased due to formation of pore blockage and denser cake layer. As a final result, PP nanocomposite membrane showed better antifouling properties compared to neat PP membrane.

Declaration of Competing Interest

We have no conflicts of interest to declare.

References

- [1] H.-Y. Yu, Y.-J. Xie, M.-X. Hu, J.-L. Wang, S.-Y. Wang, Z.-K. Xu, Surface modification of polypropylene microporous membrane to improve its antifouling property in MBR: CO₂ plasma treatment, *J. Membr. Sci.* 254 (2005) 219–227.
- [2] M. Amini, H. Etemadi, A. Akbarzadeh, R. Yegani, Preparation and performance evaluation of high-density polyethylene/silica nanocomposite membranes in membrane bioreactor system, *Biochem. Eng. J.* 127 (2017) 196–205.
- [3] Q. Lei, F. Li, L. Shen, L. Yang, B.-Q. Liao, H. Lin, Tuning anti-adhesion ability of membrane for a membrane bioreactor by thermodynamic analysis, *Bioresour. Technol.* 216 (2016) 691–698.
- [4] H. Etemadi, R. Yegani, M. Seyfollahi, The effect of amino functionalized and polyethylene glycol grafted nanodiamond on anti-biofouling properties of cellulose acetate membrane in membrane bioreactor systems, *Sep. Purif. Technol.* 177 (2017) 350–362.
- [5] R.A. Damodar, S.-J. You, H.-H. Chou, Study the self cleaning, antibacterial and photocatalytic properties of TiO₂ entrapped PVDF membranes, *J. Hazard. Mater.* 172 (2009) 1321–1328.
- [6] A. Zare, A.-K. Bordbar, A. Razmjou, F. Jafarian, The immobilization of *Candida rugosa* lipase on the modified polyethersulfone with MOF nanoparticles as an excellent performance bioreactor membrane, *J. Biotechnol.* 289 (2019) 55–63.
- [7] Ö. Çınar, H. Hasar, C. Kinaci, Modeling of submerged membrane bioreactor treating cheese whey wastewater by artificial neural network, *J. Biotechnol.* 123 (2006) 204–209.
- [8] F. Fan, H. Zhou, Interrelated effects of aeration and mixed liquor fractions on membrane fouling for submerged membrane bioreactor processes in wastewater treatment, *Environ. Sci. Technol.* 41 (2007) 2523–2528.
- [9] I. Ivanovic, T. Leiknes, Impact of aeration rates on particle colloidal fraction in the biofilm membrane bioreactor (BF-MBR), *Desalination* 231 (2008) 182–190.
- [10] F. Meng, F. Yang, B. Shi, H. Zhang, A comprehensive study on membrane fouling in submerged membrane bioreactors operated under different aeration intensities, *Sep. Purif. Technol.* 59 (2008) 91–100.
- [11] M. Ahsani, R. Yegani, Study on the fouling behavior of silica nanocomposite modified polypropylene membrane in purification of collagen protein, *Chem. Eng. Res. Des.* 102 (2015) 261–273.
- [12] S. Taghaddosi, A. Akbari, R. Yegani, Preparation, characterization and antifouling properties of nanoclays embedded polypropylene mixed matrix membranes, *Chem. Eng. Res. Des.* 125 (2017) 35–45.
- [13] M. Fonouni, H. Etemadi, R. Yegani, S. Zarin, Fouling characterization of TiO₂ nanoparticle embedded polypropylene membrane in oil refinery wastewater treatment using membrane bioreactor (MBR), *Desalin. Water Treat.* 90 (2017) 99–109.
- [14] A. Khalid, A. Abdel-Karim, M.A. Atieh, S. Javed, G. McKay, PEG-CNTs nanocomposite PSU membranes for wastewater treatment by membrane bioreactor, *Sep. Purif. Technol.* 190 (2018) 165–176.
- [15] T. Ueda, K. Hata, Y. Kikuoka, O. Seino, Effects of aeration on suction pressure in a submerged membrane bioreactor, *Water Res.* 31 (1997) 489–494.
- [16] A. Ding, H. Liang, G. Li, N. Derlon, I. Szivak, E. Morgenroth, W. Pronk, Impact of aeration shear stress on permeate flux and fouling layer properties in a low pressure membrane bioreactor for the treatment of grey water, *J. Membr. Sci.* 510 (2016) 382–390.
- [17] M. Safarpour, A. Khataee, V. Vatanpour, Effect of reduced graphene oxide/TiO₂ nanocomposite with different molar ratios on the performance of PVDF ultrafiltration membranes, *Sep. Purif. Technol.* 140 (2015) 32–42.
- [18] S. Hoseinpour, Y. Jafarzadeh, R. Yegani, S. Masoumi, Embedding neat and carboxylated nanodiamonds into polypropylene membranes to enhance antifouling properties, *Polyolefins Journal* 6 (2019) 63–74.
- [19] A. Charfi, N.B. Amar, J. Harmand, Analysis of fouling mechanisms in anaerobic membrane bioreactors, *Water Res.* 46 (2012) 2637–2650.
- [20] A. Córdova, C. Astudillo, C. Guerrero, C. Vera, A. Illanes, Assessment of the fouling mechanisms of an ultrafiltration membrane bioreactor during synthesis of galacto-oligosaccharides: Effect of the operational variables, *Desalination* 393 (2016) 79–89.
- [21] T.-H. Bae, T.-M. Tak, Effect of TiO₂ nanoparticles on fouling mitigation of ultrafiltration membranes for activated sludge filtration, *J. Membr. Sci.* 249 (2005) 1–8.
- [22] F. Shi, J. Ma, P. Wang, Y. Ma, Effect of quenching temperatures on the morphological and crystalline properties of PVDF and PVDF-TiO₂ hybrid membranes, *J. Taiwan Inst. Chem. Eng.* 43 (2012) 980–988.
- [23] Y. Jafarzadeh, R. Yegani, Analysis of fouling mechanisms in TiO₂ embedded high density polyethylene membranes for collagen separation, *Chem. Eng. Res. Des.* 93 (2015) 684–695.
- [24] V. Vatanpour, R.S.E. Naeeni, A. Ghadimi, A. Karami, B. Sadatnia, Effect of detonation nanodiamond on the properties and performance of polyethersulfone nanocomposite membrane, *Diam. Relat. Mater.* 90 (2018) 244–255.
- [25] L. De Temmerman, T. Maere, H. Temmink, A. Zwijnenburg, I. Nopens, The effect of fine bubble aeration intensity on membrane bioreactor sludge characteristics and fouling, *Water Res.* 76 (2015) 99–109.
- [26] O.P. Prat, J.J. Ducoste, Modeling spatial distribution of floc size in turbulent processes using the quadrature method of moment and computational fluid dynamics, *Chem. Eng. Sci.* 61 (2006) 75–86.
- [27] V. Vatanpour, S.S. Madaeni, A.R. Khataee, E. Salehi, S. Zinadini, H.A. Monfared, TiO₂ embedded mixed matrix PES nanocomposite membranes: influence of different sizes and types of nanoparticles on antifouling and performance, *Desalination* 292 (2012) 19–29.
- [28] A. Behboudi, Y. Jafarzadeh, R. Yegani, Preparation and characterization of TiO₂ embedded PVC ultrafiltration membranes, *Chem. Eng. Res. Des.* 114 (2016) 96–107.
- [29] W. Zhang, W. Liang, G. Huang, J. Wei, L. Ding, M.Y. Jaffrin, Studies of membrane fouling mechanisms involved in the micellar-enhanced ultrafiltration using blocking models, *RSC Adv.* 5 (2015) 48484–48491.
- [30] J.-S. Park, K.-M. Yeon, C.-H. Lee, Hydrodynamics and microbial physiology affecting performance of a new MBR, membrane-coupled high-performance compact reactor, *Desalination* 172 (2005) 181–188.
- [31] C. Wang, W.-N. Chen, Q.-Y. Hu, M. Ji, X. Gao, Dynamic fouling behavior and cake layer structure changes in nonwoven membrane bioreactor for bath wastewater treatment, *Chem. Eng. J.* 264 (2015) 462–469.